

Analysis of complexes of inhibitors with *Cryptosporidium hominis* DHFR leads to a new trimethoprim derivative

Veljko M. Popov,^a David C. M. Chan,^a Yale A. Fillingham,^a W. Atom Yee,^{a,†}
Dennis L. Wright^b and Amy C. Anderson^{b,*}

^aDepartment of Chemistry, Dartmouth College, Hanover, NH 03755, USA

^bDepartment of Pharmaceutical Sciences, University of Connecticut, Storrs, CT 06269, USA

Received 3 April 2006; revised 16 May 2006; accepted 16 May 2006

Available online 5 June 2006

Abstract—Cryptosporidiosis, an opportunistic infection affecting immunocompromised patients, the elderly, and children, is still an untreatable disease since the causative agent, *Cryptosporidium hominis*, is essentially resistant to all clinically used antimicrobial agents. In order to accelerate the design of new potent and selective inhibitors targeting dihydrofolate reductase of *C. hominis* (ChDHFR), we determined the structural basis for the potency of existing DHFR inhibitors using superpositions of the structure of ChDHFR with other species and analysis of active site complexes of ChDHFR bound to ligands exhibiting a wide range of IC₅₀ values. This information was used to develop an accurate docking model capable of identifying potent inhibitors in silico. A series of C7-trimethoprim derivatives, designed to exploit a unique pocket in ChDHFR, was synthesized and evaluated; 7-ethyl TMP has four times higher activity than TMP against ChDHFR.

© 2006 Elsevier Ltd. All rights reserved.

Cryptosporidiosis is an opportunistic infection caused by the parasitic protozoan, *Cryptosporidium hominis*, also classified as a class B biodefense pathogen. Cryptosporidiosis, for which there are no effective therapies, causes wasting disease in immune-compromised patients, the elderly, and children. Dihydrofolate reductase (DHFR) is a major drug target for this family of parasitic protozoa,¹ which also includes Plasmodium, the causative agent of malaria. DHFR is an important component of the folate biosynthetic pathway, responsible for providing the DNA base, dTMP. Alarmingly, none of the clinically used DHFR inhibitors including trimethoprim (TMP) and pyrimethamine (PYR) show any efficacy against *C. hominis* DHFR (ChDHFR), presumably due to the structural differences in the enzyme. To address this problem, several compounds were tested² with in vitro inhibition assays and although some of them were potent, none have been introduced to clinical use.

Keywords: *Cryptosporidium hominis*; Dihydrofolate reductase; Diaminopyrimidine; Docking.

* Corresponding author. Tel.: +1 860 486 6145; fax: +1 860 486 6857; e-mail: Amy.Anderson@uconn.edu

† Present address: Department of Chemistry, Santa Clara University, Santa Clara, CA 95053, USA.

In order to design potent and selective ChDHFR inhibitors, we first superposed ChDHFR with other DHFR enzymes bound to TMP and PYR, and determined the structural features of ChDHFR that explain the poor binding of TMP and PYR. We then developed a structure–activity relationship (SAR) for ChDHFR using a docking method based on ensembles of ChDHFR structures and complexes of 30 ligands with a wide range of IC₅₀ values. Based on the results of these studies, we proposed several TMP derivatives predicted to have increased activity toward ChDHFR. An efficient synthetic route to the TMP derivatives and their evaluation resulted in a better inhibitor that occupies a unique pocket as predicted by the structural analysis.

Sequence and structural alignments of ChDHFR (PDB ID: 1QZF³) with DHFR of other species revealed why several clinically used DHFR inhibitors fail to inhibit ChDHFR. Both pyrimethamine (Fig. 1), which has high binding affinity for *Plasmodium falciparum* DHFR (PfDHFR), and a dibenzazepine inhibitor, compound 4,⁴ which has potent activity against *Pneumocystis carinii* DHFR (PcDHFR), exhibit very low potency against ChDHFR (Table 1).

Superposition of modeled complexes of ChDHFR:TMP, ChDHFR:4, or ChDHFR:PYR with

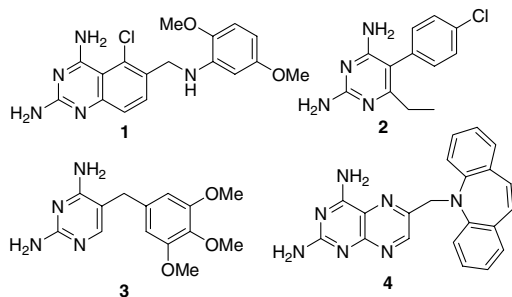


Figure 1. The most potent compound (1) docked to ChDHFR ($IC_{50} = 6.5$ nM), pyrimethamine (PYR) (2), trimethoprim (TMP) (3), and a dibenzazepine inhibitor (4).

Table 1. IC_{50} values

IC_{50}^a (μ M)	ChDHFR	PfDHFR	PcDHFR
PYR (2)	≥ 1000	0.08	N/D
TMP (3)	14	0.01	12
4	119	N/D	0.21

N/D, not determined.

^a IC_{50} values for ChDHFR were determined in our laboratory using standard spectrophotometric assays;⁵ values for PfDHFR:PYR⁶ and PcDHFR⁴ as well as a K_i value for PfDHFR:TMP⁷ were determined as described.

crystal structures of PcDHFR:TMP (1DYR⁸), PcDHFR:4 (1KLK⁹), and PfDHFR (C59R/S108N):PYR (1J3J⁶) confirmed the high structural homology of the residues that bind the 2,4-diaminopyrimidine ring and the linker regions. However, there are significant variations in the residues involved in binding the substituted phenyl rings that may relate to differences in ligand binding (Table 2); these differences will be discussed in more detail.

Leu 33 in ChDHFR narrows the pocket and restricts the size of a substituent that can be placed at the C6 position of the pyrimidine ring. Rigid superposition of ChDHFR and PfDHFR bound to pyrimethamine reveals the steric hindrance of pyrimethamine's ethyl and chlorine substituents with Leu 33 and Ile 62 of ChDHFR, respectively (Fig. 2). In PfDHFR, Met 55 adopts a rotamer conformation that allows it to avoid steric hindrance with the ethyl group.

The phenyl-binding pocket in ChDHFR is more superficial (Fig. 3) since ChDHFR lacks a loop analogous to Pro 66-Phe 69 of PcDHFR that makes many van der Waals and π -stacking interactions. In ChDHFR, the shallower phenyl-binding pocket appears to require

Table 2. Comparison of key residue differences in DHFR active sites

ChDHFR	PfDHFR	PcDHFR	Flag
Leu 33	Met 55	Ile 33	Leu 33—PYR
Absent	Pro 113	Pro 66	Absent—TMP, 4
Absent	Phe 116	Phe 69	Absent—TMP, 4
Cys 113	Ile 164	Ile 123	Cys 113—Reduced van der Waals

Flag column indicates a compound has a lower affinity for ChDHFR due to the combination of amino acids.

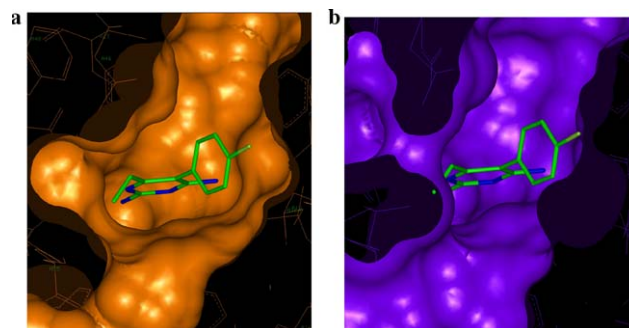


Figure 2. (a) Connolly surface of PfDHFR (gold) and pyrimethamine; (b) Modeled Connolly surface of ChDHFR (purple) with pyrimethamine. Note the ethyl group of pyrimethamine protruding into the surface of Leu 33 and the chlorine atom touching the surface of Ile 62.

smaller substituents on the phenyl ring. Compounds with halogens at the 3' and 4' positions and those with methoxy groups at the 2' and 5' positions (e.g., 1) (see III-5, III-6 and V-16 in reference²) are more potent than compounds with methoxy groups at the 3', 4', and 5' positions (see V-6, V-7, and V-9 in reference²).

Due to the difference in their volumes and conformations, the substitution of Ile 125 of PcDHFR (or Ile 164 of PfDHFR) by Cys 113 (in ChDHFR) widens the latter's linker-binding region (Fig. 4). This pocket can be occupied by the substituent on C5 of a quinazolinone ring (R^1 in Scheme 1) (e.g., 1) or by the substituent on a linker region (R^2 or R^4 in the TMP example). It is worth noting that the higher activity of the compounds with methylated linkers such as $R^2=CH_3$ or $R^3=CH_3$ may be due to the improved van der Waals interactions or to the restriction of the ligands' conformational freedom.

Next, we wanted to examine whether ligands with higher potency, but unavailable in the clinic, avoided interactions with Leu 33 and created additional van der Waals interactions in the area of the absent loop or with Cys 113. We developed an accurate and reliable method to dock inhibitors with a wide range of IC_{50} values in the ChDHFR active site using the crystal structure of the enzyme (PDB ID:1QZF³), a flexible protein model available in the program, Flo98¹⁰, and ensemble averaging.¹¹ To ensure that docking results accurately predict the affinities of novel compounds, our docking method was refined against a set of 30 known ChDHFR inhibitors, all of which had a general scaffold containing a 2,4-diaminopyrimidine, a linker region, and a substituted phenyl group (representative compounds are shown in Fig. 1). Using three independent energy terms: electrostatic (E_{est}), van der Waals (E_{vdw}), and structural complementarity (E_{cnt}), from the docking scores to estimate the $\log IC_{50}$ according to the equation: $\log IC_{50} = 18.379 + 0.296 \times E_{vdw} + 0.281 \times E_{est} + 0.206 \times E_{cnt}$, we achieved a reasonable correlation ($R^2 = 72.9\%$) between the scores of the docked protein:ligand complexes and the measured IC_{50} values, thereby validating the docked poses for these inhibitors.

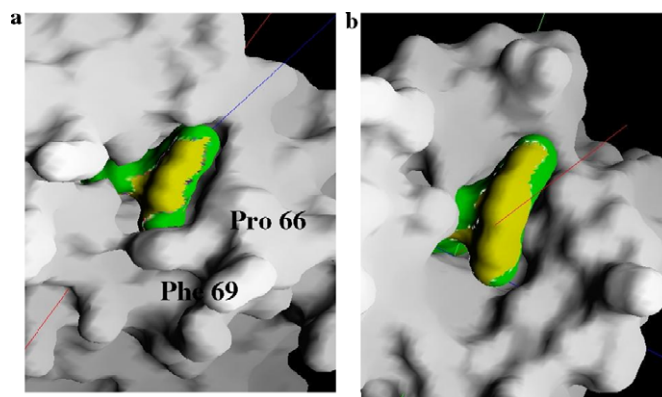


Figure 3. (a) Compound **4** in PcDHFR; (b) Compound **4** in ChDHFR. The buried surface of the ligand is colored green and the non-buried surface is colored yellow.

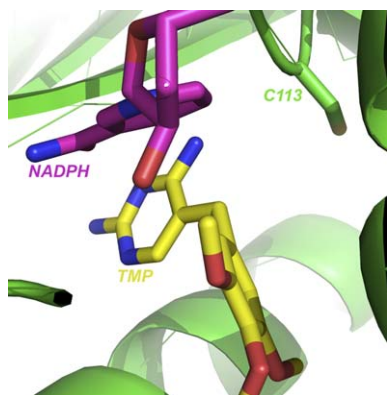
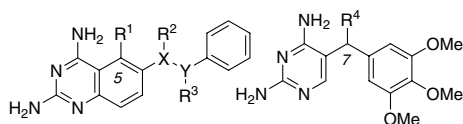


Figure 4. The pocket created by Cys 113. TMP (yellow) and NADPH (purple) are also shown.



Scheme 1. A general scaffold for the linker region of quinazoline ligands. Position 5 is noted; X or Y can be C or N; positions where substitutions occur are also noted. Also shown is a scaffold for TMP ligands with C7 noted.

For all 30 ligands, we found that E_{est} is the single best predictor of ligand activity ($R^2 = 0.4$ between E_{est} and $\log IC_{50}$). A salt bridge between the 2,4-diaminopyrimidine ring and Asp 32 is probably the major contributor of the electrostatic energy; achieving the proper orientation of the ring to form these bonds is critical. Structural complementarity between the ligand and the active site is also important, as ligands that either have steric interactions with the active site or do not adequately occupy the site have increased E_{cnt} values.

Analysis of the docked poses of potent inhibitors reveals that the 2,4-diaminopyrimidine ring assumes the same orientation in the ChDHFR active site as observed in corresponding crystal structures, with good geometry between the ring and Asp 32 as well as hydrophobic interactions between the ring and Phe 36, Val 9, Val

10, and Leu 33. The phenyl ring of most of the ligands was positioned in one of two major conformations in the active site, in either an ‘up’ conformation, defined by residues Leu 25, Thr 58, Ser 61, and Ile 62, or a ‘down’ conformation, defined by residues Leu 33 and Leu 67 (Fig. 5).

The effects of the three unique features observed in the superposition of ChDHFR with other species were obvious in the docking study. Potent compounds often have a bicyclic diaminopyrimidine ring, which avoids steric conflict with Leu 33, yet maximizes van der Waals contacts. Potent compounds were also usually larger, forming compensating van der Waals contacts for those lost by the absence of the loop at the active site. Finally, potent compounds often contained a substituent at C5 of the quinazoline that interacted with Cys 113.

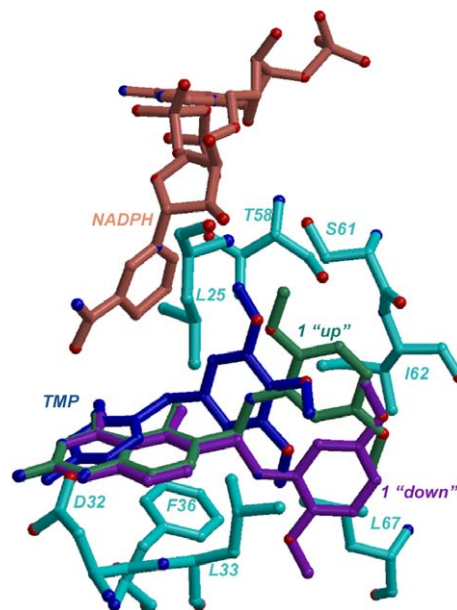


Figure 5. Interactions of compound **1** and TMP (**3**) with ChDHFR (cyan). TMP is shown in blue, the ‘up’ conformation of **1** is shown in green, and the ‘down’ conformation of **1** is shown in purple. For clarity, only one conformation of TMP is shown.

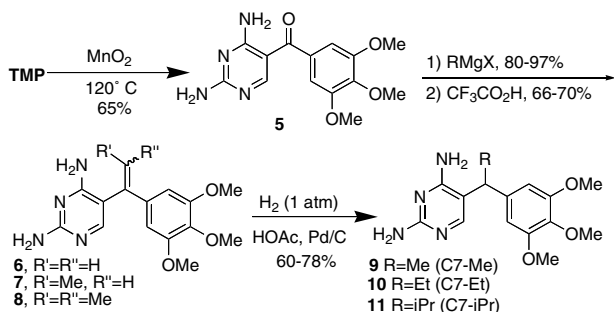
Conversely, a comparison of the most potent compound (**1**) with TMP (compound **3**; 1000-fold less potent) (Fig. 5) shows that TMP has much less favorable contact energies, most likely due to a lack of optimization of the interactions of the trimethoxyphenyl ring and the linker region. Although it adopts a similar binding orientation, the single pyrimidine ring and shorter linker region do not extend the trimethoxyphenyl ring to fully occupy the hydrophobic pockets visualized with complexes of compound **1**.

In order to validate hypotheses presented by our structural analysis, we docked, synthesized, and evaluated a series of compounds that should utilize the unique pocket created by the substitution of Ile 164 (PfDHFR) by Cys 113. These compounds served also as a test set to validate the predictions made from the docking study. A small library of C7-TMP analogs, with both R and S stereochemistry, was constructed in silico and docked into the ChDHFR active site. 7-Ethyl TMP (R) was predicted to be the most potent, with the sum of E_{vdw} , E_{est} , and E_{cnt} equal to -58.46 kJ/mol. In comparison, the energies of 7-methyl TMP and 7-isopropyl TMP were -56.85 and -56.98 , respectively.

A versatile synthetic route, presented here, provided access to a variety of C7-derivatized TMP analogs which could, in principle, be used for the design of larger libraries of compounds that share the TMP scaffold (Scheme 2).^{12–14} 7-Ethyl TMP was synthesized (as a racemic mixture) along with two related analogs, 7-Me TMP¹⁵ and 7-isopropyl TMP, both of which had higher docking energies and served as negative controls.

Benzylic oxidation of commercially available TMP was performed at elevated temperatures with activated manganese dioxide to give the ketone **5**. Addition of an excess of the Grignard reagent led to the tertiary carbinol that was subsequently dehydrated to give the alkene **6–8** in good yield. Catalytic hydrogenation over palladium on carbon produced the final analogs **9–11** for evaluation.

Each of the analogs was tested in a spectrophotometric enzyme assay.⁵ Racemic 7-ethyl TMP has an IC_{50} value of 4.2 μ M against ChDHFR, 7-Me-TMP has a value of 340 μ M, and 7-isopropyl TMP has a value greater than 100 μ M. The IC_{50} for the racemic mixture of 7-ethyl TMP is four times lower than that for TMP (14 μ M)



Scheme 2. Synthesis of C7-substituted analogs of trimethoprim.

but we would expect that the enantiomerically pure compound will have even higher activity. These results validated our docking methodology and identified a key design element that can be incorporated in future designs to increase potency. Substitution at this position may also increase selectivity since human DHFR has a bulkier valine at this position.

In conclusion, structural information and SAR data can be used to expedite the drug discovery process. We have superposed ChDHFR with several structures of DHFR from other species and identified three features that are unique in ChDHFR: Leu 33 restricts the active site and van der Waals interactions are reduced through the substitution of Cys 113 as well as the absence of a loop at the active site. Docking a broad range of inhibitors into the active site of ChDHFR allowed the development of an SAR model. The primary interactions that occur between ChDHFR and potent inhibitors include the canonical 2,4-diaminopyrimidine interactions, a substituted two-atom linker that interacts with Cys 113 and extends the phenyl group into two different hydrophobic pockets, and the interactions of the substituted phenyl group with those pockets. In order to experimentally test whether interactions with Cys 113 will improve the potency of a lower molecular weight compound, we docked several TMP analogs with substitutions at C7, predicted to interact with Cys 113. The synthesis and evaluation of these C7-TMP analogs has led to a derivative that is four times more potent than the parent compound.

Acknowledgment

Financial support by the National Institutes of Health (GM67542) is gratefully acknowledged.

References and notes

- Anderson, A. *Drug Discovery Today* **2005**, *10*, 121.
- Nelson, R.; Rosowsky, A. *Antimicrob. Agents Chemother.* **2001**, *45*, 3293.
- O'Neil, R.; Lilien, R.; Donald, B.; Stroud, R.; Anderson, A. *J. Biol. Chem.* **2003**, *278*, 52980.
- Rosowsky, A.; Cody, V.; Galitsky, N.; Fu, H.; Papoulis, A.; Queener, S. *J. Med. Chem.* **1999**, *42*, 4853.
- Anderson, A. *Acta Crystallogr., Sect. F* **2005**, *F61*, 258.
- Yuvaniyama, J.; Chitnumsub, P.; Kamchonwongpaisan, S.; Vanichtanankul, J.; Sirawaraporn, W.; Taylor, P.; Walkinshaw, M.; Yuthavong, Y. *Nat. Struct. Biol.* **2003**, *10*, 357.
- Sirichaiwat, C.; Intaradom, C.; Kamchonwongpaisan, S.; Vanichtanankul, J.; Thebtaranonth, Y.; Yuthavong, Y. *J. Med. Chem.* **2004**, *47*, 345.
- Champness, J.; Achari, A.; Ballantine, S.; Bryant, P.; Delves, C.; Stammers, D. *Structure* **1994**, *2*, 915.
- Cody, V.; Galitsky, N.; Luft, J.; Pangborn, W.; Rosowsky, A.; Queener, S. *Acta Crystallogr., Sect. D* **2002**, *D58*, 946.
- McMartin, C.; Bohacek, R. *J. Comput. Aided Mol. Des.* **1997**, *11*, 333.
- Manuscript submitted. Briefly, the active site was prepared by adding hydrogens to NADPH and residues within 11 Å of the ligand. Limited flexibility (according to Flo98) was

allowed for these active site residues, the nicotinamide and ribose of NADPH. The model of ChDHFR was subjected to a 1000-step Monte-Carlo docking search followed by a 20-step simulated annealing run. The lowest energy conformer from this search was used in future docking searches. The 30 ligands were protonated at N1 and docked in the prepared site using 500 Monte-Carlo steps followed by energy minimization. Each docking run yielded the 25 lowest energy conformers described by five energy values: the internal energy of the ligand (E_{lig}), the internal energy of the active site residues (E_{sh}) in addition to electrostatic (E_{est}), van der Waals (E_{vdw}), and contact (E_{cnt}) energies. We did not include E_{lig} or E_{sh} in the regression line since E_{lig} is calculated by molecular mechanics in vacuo and has limited accuracy. E_{sh} was omitted because the limited flexibility allowed during docking permitted some residues to move toward the shell,

accumulating energy penalties. It is assumed that in solution the shell would accommodate the slight changes of the residues and therefore the additional penalties are overestimated and inaccurate. Average values of three independent energy terms E_{est} , E_{vdw} , and E_{cnt} were used to calculate the theoretical $\log\text{IC}_{50}$ using the formula obtained from the multivariable linear regression line equation.

12. Brossi, A.; Grunberg, E.; Hoffer, M.; Teitel, S. *J. Med. Chem.* **1971**, *14*, 58.
13. Hess, S.; Dolker, M.; Haferburg, D.; Kertscher, H.; Matysik, F.; Ortwein, J.; Teubert, U.; Zimmermann, W.; Eger, K. *Pharmazie* **2001**, *56*, 306.
14. Nordholm, L.; Dalgaard, L. *Arch. Pharmacy. Org. Chem. Sci. Ed.* **1983**, *11*, 1.
15. Gangjee, A.; Lin, X.; Queener, S. E. *J. Heterocycl. Chem.* **2003**, *40*, 507.